Fibers and Polymers 2013, Vol.14, No.7, 1118-1127 DOI 10.1007/s12221-013-1118-z

Extraction of Cellulose Nanowhiskers from Natural Fibers and Agricultural Byproducts

Leandro N. Ludueña*, Antonella Vecchio[1], Pablo M. Stefani[1], and Vera A. Alvarez

Composite Materials Group, National Research Institute of Materials Science and Technology, National Research Council, National University of Mar del Plata, Mar del Plata, Argentina
[1]*Ecomaterials Group, National Research Institute of Materials Science and Technology, National Research Council, National University of Mar del Plata, Mar del Plata, Argentina*
(Received October 15, 2012; Revised December 21, 2012; Accepted December 30, 2012)

Abstract: In this work the feasibility of extracting cellulose from cotton, sisal and flax fibers, corn stover and rice husk by means of usual chemical procedures such as acid hydrolysis, chlorination, alkaline extraction, and bleaching was analyzed. Cellulose nanowhiskers from these sources, and from commercial cellulose, were produced by the acid hydrolysis of the obtained celluloses. The final products were characterized by means of Thermogravimetric Analysis (TGA), Infrared Spectroscopy (FTIR), X-ray Diffraction (XRD), Scanning Electronic Microscopy (SEM) and Atomic Force Microscopy (AFM). The chemical procedure used to obtain cellulose nanowhiskers was effective in all cases but differences on the thermal stability, chemical composition, crystallinity and morphology were found due to the dissimilar nature of the different sources. Thus, this work demonstrates that the morphology and physical properties of cellulose nanowhiskers synthesized by the same conditions are strongly dependent on their source.

Keywords: Cellulose, Natural fibers, Extraction procedures, Characterization, Cellulose nanowhiskers

Introduction

Cellulose is the main component of several natural fibers and agricultural byproducts such as sisal, cotton, and flax fibers, corn stover and rice husk within others. The α-cellulose percent content of these materials is 60-67, 90, 62-72, 38-40 and 28-36, respectively [1-3]. The structure of the natural fiber consist on cellulose, which awards the mechanical properties of the complete natural fiber, ordered in microfibers enclosed by the other two main components: hemicellulose and lignin [4]. Cellulose microfibers (CMF) can be found as intertwined microfibers in the cell wall (2-20 μm diameter and 100-40,000 nm long depending on it source) [5]. It is a linear polymer of β-(1→4)-D-glucopyranose units. The mechanical properties of CMF depend on the cellulose polymorph present named cellulose I, II, III and IV, being type I the one showing better mechanical properties. Hemicellulose is composed of different types of cycled saccharides such as xylose, mannose and glucose, among others. It forms a highly branched random structure and it is mainly amorphous [6]. Lignins are amorphous polymers formed by phenyl-propane units. They mainly consist of aromatic units such as guaiacyl, syringyl and phenylpropane [7]. There are a great number of potential uses of CMF within different industries. As a result, it has created an important focus for researcher's interest. On this field, CMF production from agro-resources has become really significant. It generally involves fibers treatment with alkalis or bisulphites to separate the lignin and to extract the hemicelluloses [8,9].

As well as these microfibers, there exist nanowhiskers (composed by cellulose) with diameters of 5-50 nm and lengths of several millimeters conformed by nanocrystalline domains and amorphous regions [5]. A controlled acid hydrolysis can separate both regions driving to crystalline domains with an elastic modulus of 150 GPa, which is higher than that of the S-glass (85 GPa) and Aramid fibers (65 GPa) [7]. In addition, it can be found in the literature [7,12] that cellulose nanowhiskers (CNW) have improved mechanical performances in comparison with CMF. Cellulose nanowhiskers have been obtained by the acid hydrolysis of cotton [13], sisal [8] and flax fibers [14] and rice husk [15]. Corn stover has been widely studied for bioenergy applications such as bioethanol and biodiesel due to its wide availability over other agricultural byproducts [16,17]. On the other hand, CNW production from corn stover was not previously reported.

Because of their good mechanical properties, the production of CNW has generated a great deal of interest as a source of nanometer-sized reinforcement. In the last years these fibers also attracted much attention due to environmental concerns especially as the reinforcement of bio-degradable polymers to produce fully bio-degradable nano-composites with enhanced mechanical properties [12,18-24].

As was explained above, the main components of natural fibers and agricultural byproducts are the same (cellulose, hemicellulose, lignin), but their content and physicochemical characteristics (i.e. fibril length, fibril width, microfiber angle, lumen diameter, cell wall thickness, crystallinity) are not [7]. Consequently, the same acid hydrolysis conditions may lead to CNW with dissimilar morphology and physicochemical properties depending on their source, which are crucial characteristics for the application proposed in this work. To our knowledge this analysis was not previously reported.

*Corresponding author: luduena@fi.mdp.edu.ar

Therefore, the aim of this work was to study the extraction of CMF and CNW from sisal, cotton, and flax fibers; corn stover and rice husk obtaining CNW by the same acid hydrolysis conditions characterizing the thermal stability, chemical composition, crystallinity and morphology of the raw materials and the obtained CNW focusing on their application as reinforcement for polymeric matrices. It must be taken into account that the production of CNW gives added value to these raw biomass material sources.

Experimental

Materials

Sisal fibers (Brazil), Cotton fibers (Argentina), Flax fibers (Argentina), Corn Stover (Argentina) and Rice Husk (Argentina), were used in this work. These fibers and agricultural byproducts will be called as Raw Materials (RM). Table 1 lists the content of their main components [3,8,25-27]. Commercial microcrystalline cellulose from Sigma Aldrich (USA) was used as reference for the comparative analysis.

Other reagents used were: toluene, ethanol, sodium hydroxide, buffer solution, sodium borate and potassium hydroxide (from Anedra, Argentina); hydrochloric acid, nitric acid, acetic acid and sulfuric acid (from Cicarelli, Argentina); sodium chlorite (from Fluka Chemie, Germany), sodium bisulphate (from Barker, USA). All reagents used were analytical grade.

Cellulose Extraction and Cellulose Nanowhisker Production Methods

Rice Husk Pre-treatment

Rice husk was extensively washed with distilled water to remove dust and other impurities. After successive washings, it was dried in an air-circulated oven at 100±2 °C until constant weight. Silica from rice husk was removed by a combination of alkaline treatment followed by precipitation with acid [28] as follows: Rice Husk was stirred with 3 % (w/v) KOH at weight ratio of 1:12 and boiled for 30 min; then the mixture was left overnight. The filtrate was washed twice with doubly distilled water, and 10 % (v/v) HCl was added (100 m*l*). The formed precipitate of silica was separated from organic residue. Finally, the organic residue was dried and ground to a fine power.

Table 1. Main components of the raw materials

Raw material	Cellulose (%)	Hemicellulose (%)	Lignin (%)	Silica (%)
Cotton [25]	85-90	5.7	< 2	-
Sisal [8]	50-74	10.0-14.0	8.0-11.0	-
Flax [25]	71	18.6-20.6	2.2	-
Corn stover [3]	38-40	28.0	7.0-21.0	-
Rice husk [26,27]	25-35	18.0-21.0	26.0-31.0	15.0-17.0

Cotton, Sisal and Flax Fibers, and Corn Stover Pre-treatment

Cotton, sisal and flax fibers, and corn stover were washed with distilled water several times and dried in an air-circulated oven at 100±2 °C until constant weight. Then they were chopped to an approximate length of 5-10 mm. Finally a de-waxing step was carried out: boiling in a mixture toluene/ethanol (2:1 volume/volume) in a soxhlet for 6 hours. The de-waxed fibers were then filtered, washed with ethanol for 30 minutes and dried at 100 °C until constant weight.

Extraction of Cellulose Microfibers

The CMF extraction procedure from all raw materials involved two main steps: I) Holocellulose (cellulose+hemicellulose) was obtained by boiling pre-treated raw materials in 0.7 wt% sodium chlorite solution at pH 4 for 2 h using a 1:50 fiber to liquor ratio. It was then treated with 5 % (w/v) sodium bisulphite solution at room temperature for 1 h using a 1:50 fiber to liquor ratio, followed by filtering, washing and drying at 100 °C until constant weight was reached; II) CMF were obtained by treating holocellulose with 17.5 wt% NaOH solution at room temperature for 8 h using a 1:50 fiber to liquor ratio, filtering, washing and drying at 100 °C until constant weight [8].

Cellulose Nanowhisker Production

CNW was prepared by the acid hydrolysis of obtained CMF. The acid hydrolysis was carried out with 60 wt% sulphuric acid (H_2SO_4) solution at 45 °C for 30 min using a 1:10 fiber to liquor ratio under continuous stirring [8].

Characterization Methods

Fourier Transformed Infrared (FTIR)

DRIFT method was followed in order to obtain FTIR spectra. 64 scans were carried out on wavenumber from 4000 to 600 cm^{-1}. The equipment used was a FTIR Genesis II.

Thermogravimetric Analysis (TGA)

Dynamic thermogravimetric measurements were performed by using a Shimadzu TGA-DTG 50 instrument. Temperature programs for dynamic tests were run from 25 to 1000 °C at a heating rate of 10 °C/min under air atmosphere (20 m*l*/min). All specimens were preconditioned at 65 % RH (relative humidity) and 20 °C.

X-ray Diffraction (XRD)

A PW1710 Diffractometer equipped with an X-ray generator (λ=0.154 nm) was used. Powder X-Ray diffractometry was carried out. Samples were scanned in 2θ ranges varying from 5 to 40 ° (1 °/min).

Scanning Electron Microscopy (SEM)

The morphology of the raw materials was analyzed by SEM micrographs with a scanning electron microscope JEOL JSM-6100 at acceleration voltage of 15 kV. Prior to the observation, the surfaces were sputter-coated with a gold layer of about 100 Å to avoid charging under the electron beam.

Atomic Force Microscopy (AFM)

The morphology of CNW was observed by AFM in a 5500 Scanning Probe Microscopy from Agilent Technologies operating in the contact mode in air. Samples were prepared by dispersing 1 mg of CNW in 20 m*l* of distilled water in an ultrasonic bath at room temperature for 30 min. A droplet of the resulting solution was cast onto a microscopy slide and dried in vacuum oven at 70 °C for 1 h. The resulting dispersed CNW were exposed to the AFM so as to collect contact mode images.

Results and Discussion

Composition and Chemical Characterization

FTIR

The chemical composition of the raw materials and CNW was analyzed by Fourier Transform Infra Red spectroscopy. The FTIR allows characterizing the chemical structure by identifying the functional groups present in each sample.

The infrared spectra of cellulose, hemicellulose and lignin have been extensively reported in the literature [6,29-32].

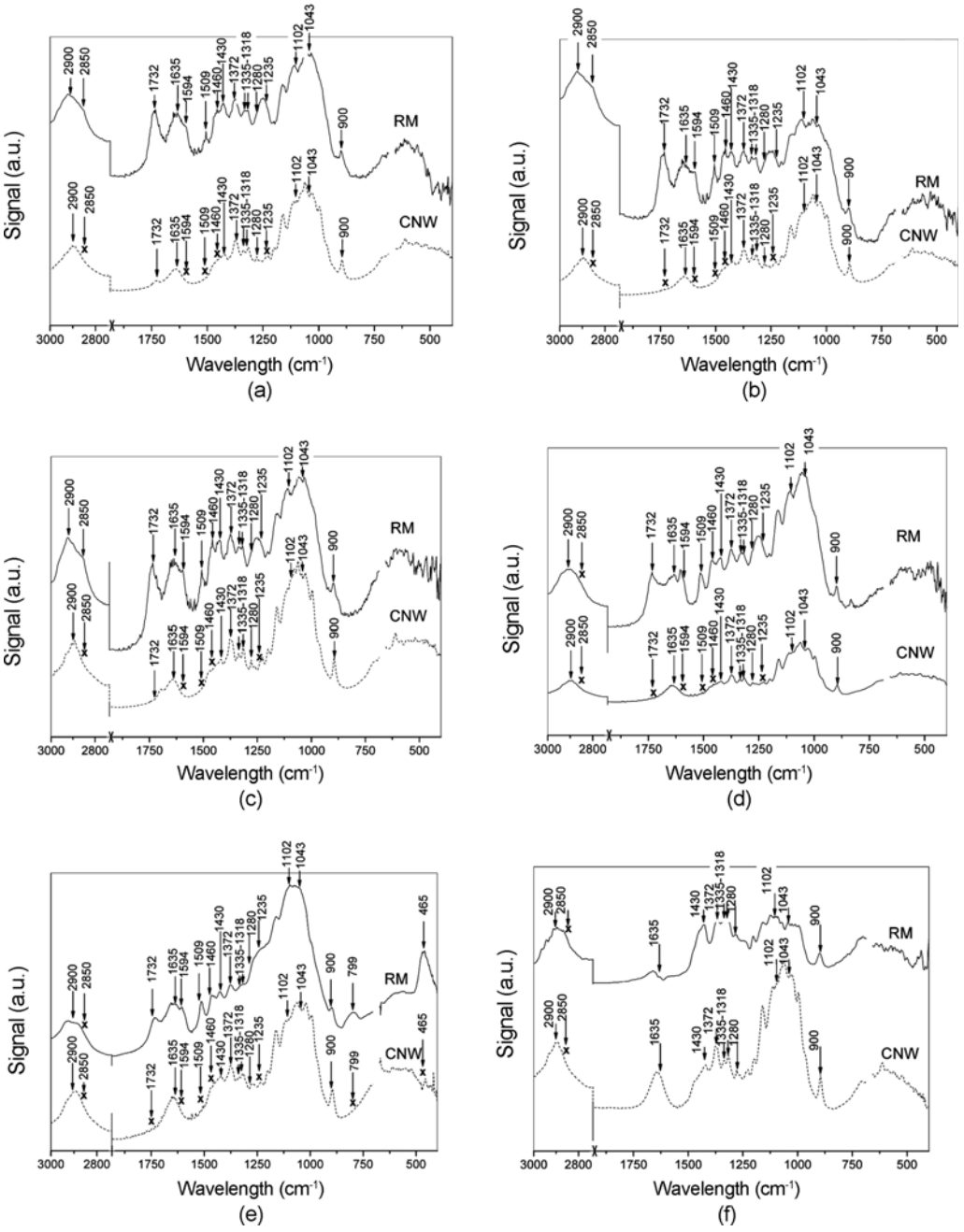

Figure 1. FTIR spectra for the raw materials (RM) and CNW; (a) sisal, (b) cotton, (c) flax, (d) corn stover, (e) rice husk, and (f) commercial.

The three materials are mainly composed of alkanes, esters, aromatics, ketones and alcohols, with different oxygen-containing functional groups. The chemical composition of sisal [8], cotton [32] and flax fibers [32], corn stover [30] and rice husk [26,28] has been previously studied and the corresponding bands for the typical functional groups of each component of these fibers and agro-residues were previously reported [8,26,28-30,32,33]. This work deals with the removal of hemicellulose, lignin, silica (only for rice husk) and amorphous cellulose from the raw materials in order to obtain CNW. The removal of these components can be analyzed following the characteristic peaks of FTIR spectra that correspond to the functional groups of hemicellulose, lignin, silica and cellulose. Changes in the chemical structure of cellulose can be also recognized by this technique.

Figures 1(a)-(f) show the FTIR spectra for the raw materials (original fibers and original agro-residues; solid lines of the figures denoted by the letters RM); and for the obtained CNW (dash lines of the figures denoted by the letters CNW). The wavelengths for the vibration of the characteristic functional groups of hemicellulose, lignin and cellulose are clearly identified with an arrow in the spectra of the raw materials and CNW. The crosses located on the CNW spectra indicate that the band is absent. A break in the X-scale of Figures 1(a)-(f) from 1290 cm^{-1} to 2750 cm^{-1} was inserted due to the fact that no bands were present in this range.

The band observed in all cases at 1635 cm^{-1} is attributed to the OH bending of absorbed water. From Figures 1(a)-(c) it can be seen that the natural fibers (Sisal, Cotton and Flax) show a shoulder at 2850 cm^{-1} originating from the C-H stretching in lignin and waxes [34,35] which was not shown in the corresponding CNW spectra. The agro-residues (Rice Husk and Corn Stover, solid lines in Figures 1(d),(e)) and the commercial cellulose (solid line in Figure 1(f)), did not show this shoulder. The peak at 1732 cm^{-1} observed in the raw materials spectra, which corresponds to vibrations of acetyl and uronic ester groups of hemicelluloses or ester linkage of carboxylic group of the ferulic and p-coumaric acids of lignin [31], was eliminated except for CNW from Sisal and Flax that showed a reduction of this band, suggesting the presence of residual lignin and/or hemicelluloses. The vibrations at 1594 cm^{-1} (aromatic rings vibrations), 1509 (aromatic rings vibrations), 1460 cm^{-1} (C-H deformations) and 1235 cm^{-1} (guaiacyl ring breathing with stretching C=O) [34-36], that appear as shoulders or peaks in the raw materials curves, are attributed to the presence of lignin and were eliminated or significantly reduced from the CNW spectra in all cases. The vibrations related with lignin and hemicelluloses, except to that at 2850 cm^{-1}, were not observed in the spectra of the commercial cellulose (solid line in Figure 1(f)) due to the fact that these fibers were submitted to a previous step of lignin and hemicelluloses extraction performed by the supplier. The band at 1043 cm^{-1} (C-O-C stretching) related with xylans associated with hemicelluloses [37] is not clearly identified but it may be overlapped by the vibrations between 1140 cm^{-1} and 920 cm^{-1}. Renard *et al*. [38] explained that xylans are strongly bound to the cellulose because they are able to bind onto cellulose fibrils in a manner similar to the interchain bonding of the cellulose itself.

From the analysis of the characteristic functional groups of hemicelluloses and lignin it can be concluded that these components were effectively removed from the raw materials in all cases. Only CNW from Sisal and Flax presented signs of small amounts of residual lignin and/or hemicelluloses. Comparing the functional groups of cellulose for the raw materials and the corresponding CNW, a reduction of the intensity at 1102 cm^{-1} is observed in all cases which can be attributed to the transition from cellulose I to cellulose II [31]. This result will be also analyzed by XRD. On the other hand, CNW showed higher intensity and narrower bands at 900 cm^{-1} than those of the corresponding raw materials at the same wavelength. Thinner peaks at 900 cm^{-1} reflect less amorphous cellulose, which was expected since it was the role of the acid hydrolysis, while higher intensity at 900 cm^{-1} suggest that the crystalline structure changes from cellulose I to cellulose II [32]. A typical band of crystalline cellulose is that at 1280 cm^{-1} which can be observed for all CNW. In the case of the raw materials, except to commercial cellulose, this band is overlapped with the one at 1235 cm^{-1} so it could not be compared with that of the corresponding CNW. The bands at 1430 cm^{-1}, 1372 cm^{-1}, 1335 cm^{-1} and 1318 cm^{-1} occur due to COH and HCC bending vibrations and are typical of crystalline cellulose [32]. In all cases the band at 1372 cm^{-1} did not significantly change after acid hydrolysis but a reduction of the intensity of the bands at 1430 cm^{-1}, 1335 cm^{-1} and 1318 cm^{-1},corresponding to high crystalline cellulose I [32], was observed, which is a sign of absence of crystalline cellulose I form in CNW. Other authors [33] have found that the band at 2900 cm^{-1} is sensitive to changes of the amorphous regions of cellulose but no significant differences comparing the raw materials with the corresponding CNW were found in this work. Similar observations were reported by Kavkler *et al*. [32]. In the case of Rice Husk, two bands at 799 cm^{-1} and 465 cm^{-1} were observed in the spectra of the raw material. These bands are related with Si-O-Si bonds [28] that arises from the high content of silica of this agro-residue (see Table 1), but they are absent in the spectra of the corresponding CNW. This result confirms that the silica was removed by the alkaline pretreatment performed to Rice husk.

Additionally to the visual observation of the different bands, Table 2 shows a band intensity ratio named Lateral Order Index ($LOI=I_{1430}/I_{900}$) which give information about changes in crystallinity related with cellulose I [39]. The values reported in Table 2 are in the range of those found in the literature for cellulose and natural fibers from different sources [32,39]. It can be seen that the LOI values for the CNW are lower than those of the corresponding raw materials which suggests that

the crystalline structure of cellulose changes from cellulose I to cellulose II as was previously stated after the visual observation of the bands related with these components.

TGA

Due to the differences in the chemical structure between hemicellulose, cellulose and lignin, they usually decompose at different temperatures. Yang *et al*. [40] showed that during thermal analysis, cellulose decomposition started at 315 °C and persisted until 400 °C. Maximum weight loss rate was reached at 355 °C. At 400 °C almost all cellulose was pyrolyzed, and the solid residuals were relatively small (6.5 wt. %). Hemicellulose started its decomposition at 220 °C and continued up to 315 °C. The decomposition peak reached the maximum mass loss rate at 268 °C, showing a 20 wt. % of remaining solid residuals at 700 °C. Finally, they showed that lignin decomposition extended to the whole temperature range, starting well below 200 °C and persisting above 700 °C. The solid residue left from lignin pyrolysis was the highest one (46 wt. %).

The thermogravimetric analysis (TGA) allows to study the thermal stability of the materials and the derivative thermogravimetric analysis (DTGA) allows identifying the maximum weight loss rate of the components. The curves resulting from each analysis for the raw materials and CNW are

Table 2. FTIR, TGA and DTGA parameters for the raw materials and CNW

Raw materials	LOI	M (%)	Residue (%, 900 °C)	Tsh (°C)	Tα (°C)	Tβ (°C)
Sisal	1.1064	7.6	4.9	265	345	516
Cotton	1.2338	9.3	1.7	296	339	480
Flax	1.2725	7.7	2.7	300	346	496
Corn stover	2.1309	7.4	3.5	305	337	456
Rice husk	4.8127	7.1	25.7	311	330	457
Commercial	1.1262	5.6	0.7	-	329	498
CNW from						
Sisal	1.0289	4.0	2.0	300	332	410
Cotton	1.0353	7.3	1.2	260	317	500
Flax	1.0887	5.8	2.5	263	333	484
Corn stover	0.9382	7.4	3.9	-	322	488
Rice husk	0.8368	4.6	1.5	-	314	426
Commercial	1.1581	8.7	3.0	-	349	466

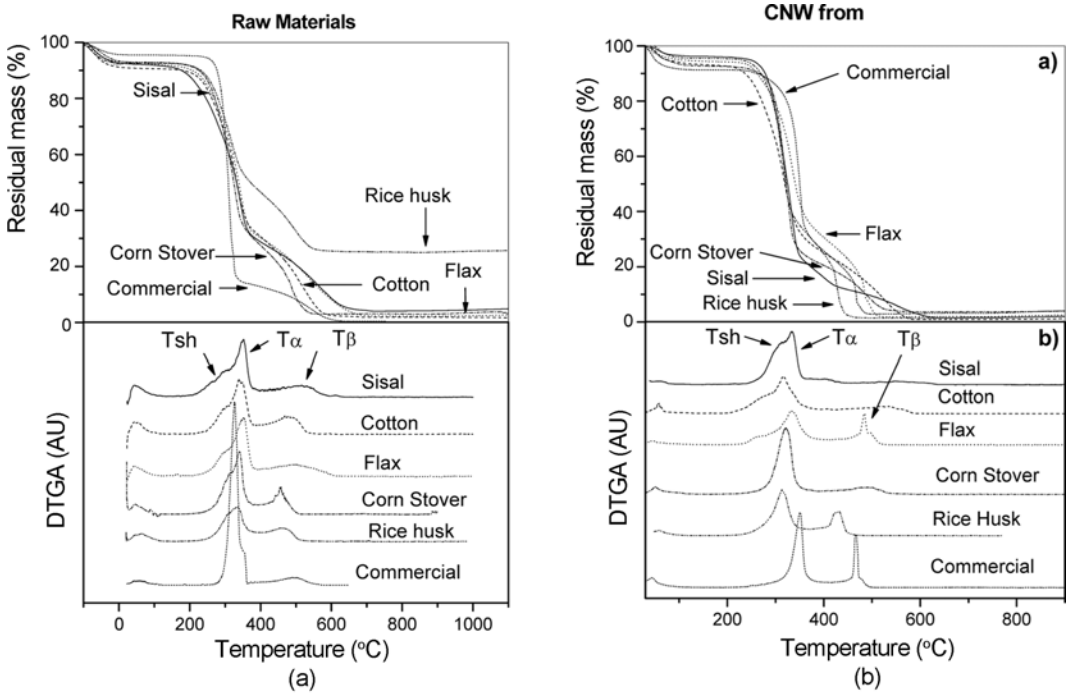

Figure 2. TGA and DTGA curves for (a) raw materials and (b) CNW.

shown in Figures 2(a),(b), respectively.

Table 2 also shows the parameters calculated from the TGA and DTGA analysis for the raw materials and the obtained CNW, respectively.

The parameters shown in Table 2 were calculated as follows. M is the moisture content of the samples calculated from the TGA curves (mass loss at 150 °C); Tsh is the mean value of the range of temperatures of the shoulder located on the left of the main peak (DTGA curves); Tα is the temperature of the maximum of the main peak (DTGA curves) and Tβ is the temperature of the maximum of the peak located above 350 °C (DTGA curves). See Figures 2(a),(b) for the location of Tsh, Tα and Tβ.

Decomposition of the raw materials shows several stages, indicating the presence of different components that decompose at different temperatures. In all cases, a small weight loss was found in the range 25-150 °C due to the evaporation of water. It is well known that all of the natural fibers and the agro-residues used in this work are hydrophilic in nature; their moisture content reaches 8-12.6 % [41], which is in accordance with the values of M shown in Table 2. On the other hand, it has been demonstrated that the main components of the lignocellulosic fibers absorb water at different proportions in the following order: Hemicellulose > Accessible Crystalline Cellulose > Non-crystalline Cellulose > Lignin >>> Crystalline Cellulose [42]. The differences found on the moisture content for the raw materials are negligible, except to Commercial Cellulose, due to the balanced content of the components above mentioned. This hypothesis is supported by the results for the Commercial Cellulose that showed the lowest M value and is the only raw material that was pretreated for hemicelluloses and lignin extraction. On the other hand, comparing the M value of the raw materials with that of the corresponding CNW, it can be observed that the moisture content diminished as a consequence of hemicellulose and lignin extraction, except to the commercial one. In the latter case the M value of the Commercial Cellulose is lower than that of the corresponding CNW probably because the acid hydrolysis promotes the exposure of OH groups at the surface of the fibers.

The differences found for the M value of the CNW are not negligible. Higher values of M could be attributed to the presence of amorphous cellulose due to a partial acid hydrolysis. This hypothesis will be analyzed in the next section by means of the crystallinity index calculated by XRD.

The residual mass at 900 °C for the raw materials was in the range of 0.7-4.9 % which corresponds to ash that, in most cases, arises from the carbon content of the samples [26]. In the case of rice husk, higher residual mass at 900 °C (25.7 %) is observed due to the high content of silica of this agro-residue [27]. The residual mass at 900 °C for the CNW was slightly lower than that of the corresponding raw material as a consequence of lignin and hemicelluloses removal [43]. In the case of CNW from rice husk a significant reduction (↓24.2 %) of the residual mass at 900 °C was observed as a consequence of the pretreatment for silica extraction performed before the synthesis of CMF.

It can be seen from the DTGA analysis that in the case of the raw materials the decomposition starts at around 220 °C, which corresponds mainly to lignin and hemicellulose decomposition. The presence of a broadening on the left side of the main peak (Tα), that appears as a shoulder represented by the temperature Tsh, corresponds also to lignin and hemicellulose decomposition. Commercial Cellulose did not show this shoulder due to the pretreatment for hemicelluloses and lignin extraction performed by the supplier, which is in accordance with FTIR observations. In the case of the original sisal fibers the decomposition starts at lower temperature (around 200 °C) which can be attributed to the higher lignin content (Table 1).

Regarding CNW from sisal, cotton and flax, a small broadening on the left side of the main peak can be observed (the corresponding Tsh values are shown in Table 2). It can be attributed to a broad distribution of cellulose's molecular mass or a residual content of hemicellulose [8]. FTIR results showed a residual content of lignin and/or hemicelluloses for CNW from Sisal and Flax fibers that confirm this hypothesis. On the other hand, another hypothesis for the appearance of this shoulder arises from the work by Varhegyi *et al*. [44] who stated that the thermal degradation of cellulose with acid catalyst includes two consecutive reactions that can be described as follows. Under the catalysis of acid sulphate groups, the dehydration reaction firstly takes place at lower temperature at cellulose chain units containing these groups. The consecutive degradation reaction occurs at the cellulose chains which were not in direct contact with the catalyst or in the cellulose crystal interior [44], probably accompanied by some char residue formation. In the case of CNW from corn stover, rice husk and Commercial Cellulose a sharp peak with a maximum decomposition rate at 322 °C, 314 °C and 349 °C, respectively, was shown in Figure 2(b). In these cases there were no signs of broadening or shoulders on the left side of the main peak.

The main peak of the DTGA curves, represented by the temperature Tα, corresponds to the pyrolysis process of cellulose. In the case of the raw materials, slight differences for Tα were observed (Table 2) which may be due to the dissimilar nature of cellulose which comes from the different natural sources. In the case of CNW the differences for the Tα values were more notorious probably because the acid hydrolysis destroyed the crystalline structure of cellulose at different extents [45], i.e. cellulose changes from cellulose I to cellulose II, which was confirmed by the LOI index shown in Table 2 and will be also analyzed by XRD. On the other hand, CNW presented lower Tα than that of the corresponding raw material. In a previous work [46], we obtained similar results for CNW from cotton. Roman *et al.* [47] demonstrated that the thermal degradation of cellulose crystals containing

sulphate groups occurs at lower temperatures. They stated that the thermal degradation reactions of bacterial cellulose are catalyzed by sulfuric acid. Catalysis could either be direct through the acid molecules or indirect by promoting dehydration reactions and increasing the amount of water released. The replacement of OH groups by sulphate groups decreases the activation energy of cellulose chain degradation.

In all cases a peak above 400 °C was observed in the DTGA curves. The temperature for the maximum value of this peak was named Tβ. Matínez-Sanz *et al.* [48] stated that this peak is a consequence of the thermo-oxidation and breakdown of the charred residue that takes place in tests under air atmosphere. On the other hand, Wang *et al.* [45] studied the thermal stability of CNW from acid hydrolyzed commercial microcrystalline cellulose under nitrogen atmosphere. They also saw this peak attributing it to a second pyrolysis process related to the slow decomposition of solid residues to form the char products. They observed that this process takes place only in the presence of acid sulphate groups. CNW crystals that were complete neutralized did not show the second pyrolysis process. As was previously mentioned, in our case this peak was observed in all curves (raw materials and obtained CNW), therefore, due to the fact that the raw materials were not in contact with sulphate groups and that our test were carried out under air atmosphere, we suggest that this peak is a consequence of thermo-oxidative events as reported by Matínez-Sanz *et al.* [48].

XRD

The X-ray diffractometer was used to investigate the crystalline structure of the samples and the X-ray curves of the raw materials and the obtained CNW are shown in Figures 3(a),(b). From the X-ray curves, it was clearly observed that the X-ray diffraction patterns of the raw materials and the CNW are different. The curves of the raw materials showed two main peaks, one close to 2θ=22 ° representing the crystalline part of the materials and the other close to 2θ=16 ° representing the amorphous one. In the case of CNW three main peaks are present, the peak at 2θ=22 ° was separated into two peaks at 22 ° (cellulose I) and 20 ° (cellulose II) indicating that cellulose was transformed from cellulose I to cellulose II during the alkali extraction of CMF [26,49], which is in accordance with the FTIR and TGA analysis, and the third peak, close to 12 °, is the amorphous one. From the obtained patterns, it is possible to estimate the crystallinity index of the materials as follows [50]:

$$I_c(\%) = \frac{(I_{crystalline} - I_{amorphous})}{I_{crystalline}} \times 100 \quad (1)$$

where $I_{crystalline}$ is the intensity at 22 ° or the sum of intensities at 22 ° and 20 ° for the patterns showing only cellulose I or both cellulose I/cellulose II, respectively, and $I_{amorphous}$ is the intensity of the peak at 2 angle close to 16 ° (amorphous). The relative quantity of cellulose II with respect to cellulose I can be calculated by the following equation:

$$I_{II-I}(\%) = \frac{I_{20}}{I_{20} + I_{22}} \times 100 \quad (2)$$

Table 3 summarizes both the I_c and I_{II-I} values for all materials.

The values of the index I_{II-I} show that the transformation from cellulose I to cellulose II after the acid hydrolysis was in the range of 49-50 %. Comparing the I_c values of the raw materials it can be observed that the higher values were obtained for Sisal, Cotton and Flax probably due to the higher content of cellulose of these fibers (see Table 1). As was expected, the Commercial Cellulose showed the highest I_c value due to the fact that it was pretreated by the supplier for hemicelluloses and lignin extraction, also demonstrated by FTIR and TGA. The I_c values for the CNW are higher than those of the corresponding raw materials as a consequence of the extraction of amorphous components (lignin, hemicelluloses, amorphous cellulose). In the TGA section it was explained that the differences found for the moisture content of the CNW (M parameter, Table 2) could be attributed to the

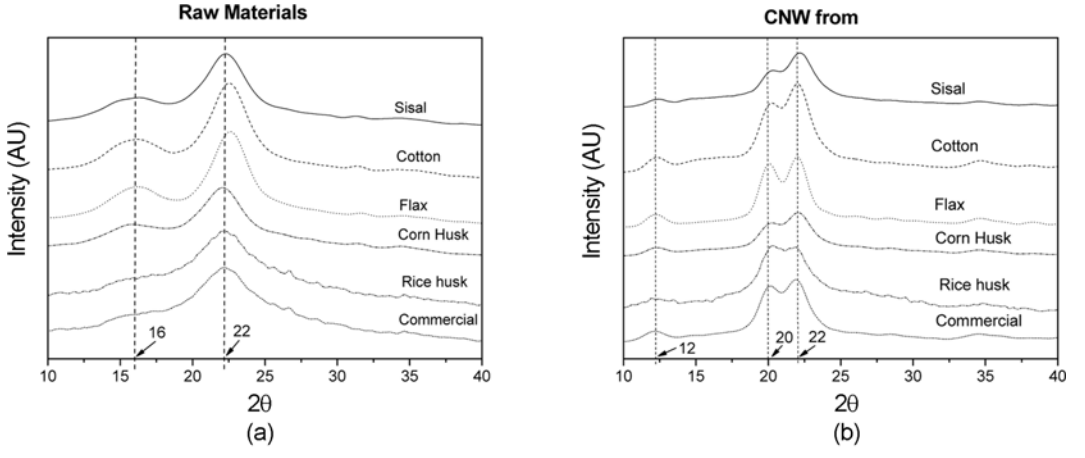

Figure 3. XRD curves for (a) raw materials and (b) CNW.

Table 3. Crystallinity index and average diameter for the raw materials and CNW

Raw materials	I_c (%)	I_{II-I} (%)	Diameter (μm)
Cotton	44.4 (Cel I)	-	130.6
Sisal	48.7 (Cel I)	-	287.5
Flax	50.3 (Cel I)	-	51.1
Corn Stover	35.1 (Cel I)	-	509.4
Rice Husk	32.0 (Cel I)	-	-
Commercial	75.0 (Cel I)	-	9.6
CNW from	I_c (%)	I_{II-I} (%)	Diameter (nm)
Cotton	94.0 (Cel I and Cel II)	38.9	73.4
Sisal	85.9 (Cel I and Cel II)	42.2	57.4
Flax	84.9 (Cel I and Cel II)	47.3	39.4
Corn stover	80.6 (Cel I and Cel II)	40.8	38.4
Rice husk	76.0 (Cel I and Cel II)	50.6	12.4
Commercial	81.7 (Cel I and Cel II)	46.6	21.7

presence of different contents of amorphous cellulose due to a partial acid hydrolysis. The I_c values of Table 3 confirm that the acid hydrolysis was not complete because they are lower than 100 %, as was expected from the values found in the literature [15,43,47,51], but the trend found for I_c is not in accordance with M probably because the crystallinity index calculated by XRD gives information about the surface of the sample and the moisture content calculated by TGA represents both surface and bulk.

Microscopic Analysis: Morphological Characterization

SEM - AFM

Figures 4(a)-(f) show the SEM and AFM micrographs of the raw materials and CNW. Diameter of at least 50 particles was measured in order to make a statistical distribution. Table 3 summarizes the obtained results.

The diameter of the raw materials was around 10-500 μm. Original Cotton, Sisal and Flax fibers and Corn Stover are composed by several cellulose microfibers with diameters in

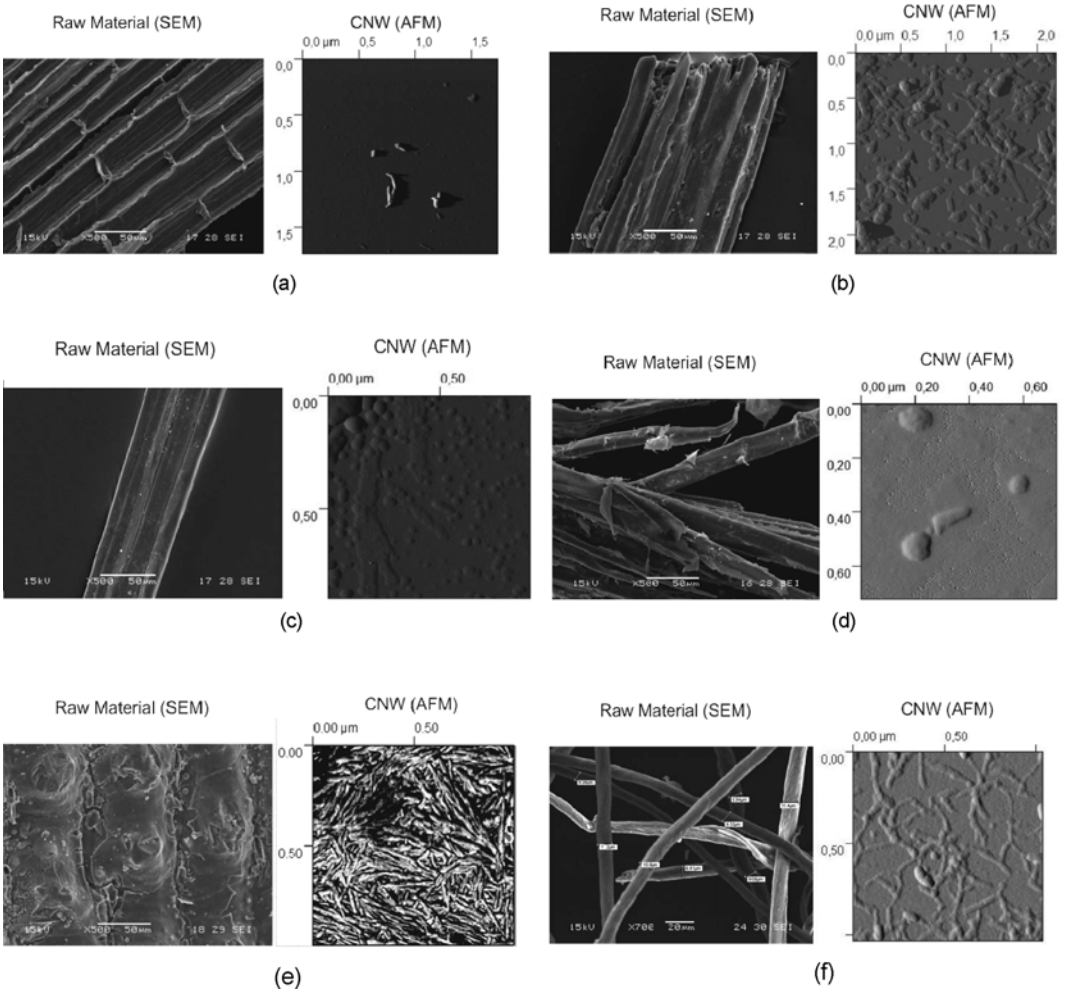

Figure 4. SEM and AFM micrographs for the raw materials and CNW; (a) sisal, (b) cotton, (c) flax, (d) corn stover, (e) rice husk, and (f) commercial.

the range of 8-12 μm which is in accordance with the diameter of the commercial cellulose microfibers shown in Figure 4(f). In their natural state, and before chemical extraction, fiber surfaces have waxes and other encrusting substances such as hemicellulose, lignin and pectin that form a thick outer layer to protect the cellulose inside [7]. The presence of encrusting substances causes the fibers to have an irregular appearance as shown in Figures 4. The picture on the left of Figure 4(e) corresponds to Rice husk showing the outer surface of lemma. It can be observed a highly roughened surface that shows ridged structures linearly arranged and punctuated with prominent domes [52]. The silica is mainly localized in the tips of the domes, whereas a lower amount of silica can be found in other regions of the lemma [52].

Regarding CNW, the lower diameter was obtained with that from Rice Husk. The length of the fibers could not be measured because it was difficult to recognize the beginning and ending of an individual fiber. Even when the length of the fibers could not be measured, it can be observed from the AFM images that the CNW from Sisal, Rice Husk and Commercial Cellulose showed lower aspect ratios. In the case of CNW from Rice Husk and Commercial Cellulose not only the aspect ratio is lower but also the diameter which make them potential candidates as reinforcement of polymer matrices.

Conclusion

It was possible to obtain CNW from all proposed sources (natural fibers, agricultural wastes and commercial cellulose). CNW from sisal and flax were the only ones that showed small amounts of lignin and hemicellulose, demonstrated by FTIR. The CNW from rice husk displayed the smallest diameter, the lowest thermal stability (Tα) and the lowest crystallinity. These results could be a consequence of the special chemical treatment performed to rice husk for silica extraction. Smaller diameter could be beneficial for applications such as reinforcement of polymeric matrices but lower thermal stability could be a problem during melt processing and lower crystallinity indicates lower degree of hydrolysis and probably poor mechanical properties of the fiber itself. All produced CNW displayed dissimilar characteristics that lied in the next ranges: 12.4-73.4 nm for the diameter, 39-51 % for cellulose II content and 76-94 % for crystallinity. Regarding the thermal stability, the peak corresponding to the pyrolysis process of cellulose was in the range of 314-349 ^{o}C. The differences found for these characteristics demonstrate that the morphology and physical properties of CNW synthesized by the same conditions are strongly dependent on their source. The optimal balance of the properties before mentioned, including morphology, should be analyzed before selecting them as reinforcement of polymeric matrices. This balance can be tuned for each source analyzing the effect of acid hydrolysis conditions (acid solution concentration, temperature, reaction time, solution/fiber ratio) on the characteristics of the obtained CNW.

Acknowledgements

Authors acknowledge to the National Research Council of Argentina (CONICET, PIP 1837), the National University of Mar del Plata (UNMdP) and the National Agency of Science and Technology of Argentina (ANPCyT) for the financial support.

References

1. K. G. Satyanarayana, G. G. C. Arizaga, and F. Wypych, *Prog. Polym. Sci.*, **34**, 982 (2009).
2. M. Kurakake, W. Kisaka, K. Ouchi, and T. Komaki, *Appl. Biochem. Biotechnol.*, **90**, 251 (2001).
3. N. Reddy and Y. Yang, *Trends in Biotechnology*, **23**, 22 (2005).
4. V. Placet, *Compos. Part-A: Appl. S.*, **40**, 1111 (2009).
5. T. Itoh and R. M. Brown, *Planta*, **160**, 372 (1984).
6. B. Xiao, X. F. Sun, and R. Sun, *Polym. Degrad. Stab.*, **74**, 307 (2001).
7. C. Baillie, "Green Composites: Polymer Composites and the Environment" (D. T. Nishino Ed.), p.49, in Abington Hall, Abington Cambridge CB1 6AH, England, Woodhead Publishing Limited: Department of Chemical Science and Engineering, Faculty of Engineering, Kobe University. 2004.
8. J. Morán, V. Alvarez, V. Cyras, and A. Vázquez, *Cellulose*, **15**, 149 (2008).
9. S. Elanthikkal, U. Gopalakrishnapanicker, S. Varghese, and J. T. Guthrie, *Carbohyd. Polym.*, **80**, 852 (2010).
10. L. Petersson and K. Oksman, *Compos. Sci. Technol.*, **66**, 2187 (2006).
11. Y. Chen, C. Liu, P. R. Chang, X. Cao, and D. P. Anderson, *Carbohyd. Polym.*, **76**, 607 (2009).
12. M. A. S. Azizi Samir, F. Alloin, and A. Dufresne, *Biomacromolecules*, **6**, 612 (2005).
13. E. de Morais Teixeira, A. Corrêa, A. Manzoli, F. de Lima Leite, C. de Oliveira, and L. Mattoso, *Cellulose*, **17**, 595 (2010).
14. E. H. Qua and P. R. Hornsby, *Plastics, Rubber and Composites*, **40**, 300 (2011).
15. S. M. L. Rosa, N. Rehman, M. I. G. de Miranda, S. M. B. Nachtigall, and C. I. D. Bica, *Carbohyd. Polym.*, **87**, 1131 (2012).
16. K. L. Kadam and J. D. McMillan, *Bioresource Technology*, **88**, 17 (2003).
17. S. Sokhansanj, A. Turhollow, J. Cushman, and J. Cundiff, *Biomass and Bioenergy*, **23**, 347 (2002).
18. A. Morin and A. Dufresne, *Macromolecules*, **35**, 2190 (2002).
19. L. Petersson, I. Kvien, and K. Oksman, *Compos. Sci.*

Technol., **67**, 2535 (2007).
20. A. Dufresne, D. Dupeyre, and M. R. Vignon, *J. Appl. Polym. Sci.*, **76**, 2080 (2000).
21. H. Lönnberg, L. Fogelström, L. Berglund, E. Malmström, and A. Hult, *Eur. Polym. J.*, **44**, 2991 (2008).
22. W. J. Orts, J. Shey, S. H. Imam, G. M. Glenn, M. E. Guttman, and J.-F. Revol, *J. Polym. Environ.*, **13**, 301 (2005).
23. J. M. Lagaron and A. Lopez-Rubio, *Trends in Food Science & Technology*, **22**, 611 (2011).
24. M. Wollerdorfer and H. Bader, *Ind. Crop. Prod.*, **8**, 105 (1998).
25. H. M. Akil, M. F. Omar, A. A. M. Mazuki, S. Safiee, Z. A. M. Ishak, and A. Abu Bakar, *Materials & Design*, **32**, 4107 (2011).
26. N. Johar, I. Ahmad, and A. Dufresne, *Ind. Crop. Prod.*, **37**, 93 (2012).
27. P. M. Stefani, D. Garcia, J. Lopez, and A. Jimenez, *J. Therm. Anal. Calorim.*, **81**, 315 (2005).
28. L. Ludueña, D. Fasce, V. Alvarez, and P. Stefani, *BioResources*, **6**, 1440 (2011).
29. H. Erdtman, *J. Polym. Sci. Part B: Polym. Lett.*, **10**, 228 (1972).
30. X. Yang, F. Ma, Y. Zeng, H. Yu, C. Xu, and X. Zhang, *International Biodeterioration & Amp; Biodegradation*, **64**, 119 (2010).
31. R. Zuluaga, J. L. Putaux, J. Cruz, J. Vélez, I. Mondragon, and P. Gañán, *Carbohyd. Polym.*, **76**, 51 (2009).
32. K. Kavkler, N. Gunde-Cimerman, P. Zalar, and A. Demšar, *Polym. Degrad. Stab.*, **96**, 574 (2011).
33. S. Y. Oh, D. I. Yoo, Y. Shin, and G. Seo, *Carbohyd. Res.*, **340**, 417 (2005).
34. P. Gañán, J. Cruz, S. Garbizu, A. Arbelaiz, and I. Mondragon, *J. Appl. Polym. Sci.*, **94**, 1489 (2004).
35. P. Gañán, R. Zuluaga, J. M. Velez, and I. Mondragon, *Macromolecular Bioscience*, **4**, 978 (2004).
36. J. X. Sun, X. F. Sun, H. Zhao, and R. C. Sun, *Polym. Degrad. Stab.*, **84**, 331 (2004).
37. F. Xu, J. X. Sun, Z. C. Geng, C. F. Liu, J. L. Ren, R. C. Sun, P. Fowler, and M. S. Baird, *Carbohyd. Polym.*, **67**, 56 (2007).
38. C. M. G. C. Renard and M. C. Jarvis, *Plant Physiology*, **119**, 1315 (1999).
39. M. Ali, A. M. Emsley, H. Herman, and R. J. Heywood, *Polymer*, **42**, 2893 (2001).
40. H. Yang, R. Yan, H. Chen, D. H. Lee, and C. Zheng, *Fuel*, **86**, 1781 (2007).
41. A. K. Bledzki, S. Reihmane, and J. Gassan, *J. Appl. Polym. Sci.*, **59**, 1329 (1996).
42. A. K. Mohanty, M. Misra, and G. Hinrichsen, *Macromol. Mater. Eng.*, **276-277**, 1 (2000).
43. R. Li, J. Fei, Y. Cai, Y. Li, J. Feng, and J. Yao, *Carbohyd. Polym.*, **76**, 94 (2009).
44. G. Varhegyi, M. J. Antal, T. Szekely, F. Till, and E. Jakab, *Energy & Fuels*, **2**, 267 (1988).
45. N. Wang, E. Ding, and R. Cheng, *Polymer*, **48**, 3486 (2007).
46. L. Ludueña, A. Vázquez, and V. Alvarez, *Carbohyd. Polym.*, **87**, 411 (2012).
47. M. Roman and W. T. Winter, *Biomacromolecules*, **5**, 1671 (2004).
48. M. Martínez-Sanz, A. Lopez-Rubio, and J. M. Lagaron, *Carbohyd. Polym.*, **85**, 228 (2011).
49. L. Y. Mwaikambo and M. P. Ansell, *J. Appl. Polym. Sci.*, **84**, 2222 (2002).
50. L. Segal, J. J. Creely, A. E. Martin, and C. M. Conrad, *Text. Res. J.*, **29**, 786 (1959).
51. E. D. M. Teixeira, D. Pasquini, A. A. S. Curvelo, E. Corradini, M. N. Belgacem, and A. Dufresne, *Carbohyd. Polym.*, **78**, 422 (2009).
52. B.-D. Park, S. G. Wi, K. H. Lee, A. P. Singh, T.-H. Yoon, and Y. S. Kim, *Biomass and Bioenergy*, **25**, 319 (2003).